RESEARCH ARTICLE

WILEY

Mutational analysis of the Hsp70 substrate-binding domain: Correlating molecular-level changes with in vivo function

Linan Xu[1] | Hong Zhang [2] | Daragh D. Cuskelly[1] | Sean Doyle[1] | Sarah Perrett [2,3] | Gary W. Jones [1,4]

[1]Department of Biology, Maynooth University, Maynooth, Ireland

[2]National Laboratory of Biomacromolecules, CAS Center for Excellence in Biomacromolecules, Institute of Biophysics, Chinese Academy of Sciences, Beijing, China

[3]University of the Chinese Academy of Sciences, Beijing, China

[4]Centre for Biomedical Science Research, School of Clinical and Applied Sciences, Leeds Beckett University, Leeds, UK

Correspondence
Gary W. Jones, Centre for Biomedical Science Research, School of Clinical and Applied Sciences, Leeds Beckett University, Portland Building, City Campus, Leeds LS1 3HE, UK.
Email: gary.jones@leedsbeckett.ac.uk

Abstract

Hsp70 is an evolutionarily conserved chaperone involved in maintaining protein homeostasis during normal growth and upon exposure to stresses. Mutations in the β6/β7 region of the substrate-binding domain (SBD) disrupt the SBD hydrophobic core resulting in impairment of the heat-shock response and prion propagation in yeast. To elucidate the mechanisms behind Hsp70 loss of function due to disruption of the SBD, we undertook targeted mutational analysis of key residues in the β6/β7 region. We demonstrate the critical functional role of the F475 residue across yeast cytosolic Hsp70-Ssa family. We identify the size of the hydrophobic side chain at 475 as the key factor in maintaining SBD stability and functionality. The introduction of amino acid variants to either residue 475, or close neighbor 483, caused instability and cleavage of the Hsp70 SBD and subsequent degradation. Interestingly, we found that Hsp70-Ssa cleavage may occur through a vacuolar carboxypeptidase (Pep4)-dependent mechanism rather than proteasomal. Mutations at 475 and 483 result in compromised ATPase function, which reduces protein re-folding activity and contributes to depletion of cytosolic Hsp70 in vivo. The combination of reduced functionality and stability of Hsp70-Ssa results in yeast cells that are compromised in their stress response and cannot propagate the [PSI^+] prion.

KEYWORDS
heat shock, Hsp70, Pep4, prion, protein cleavage, protein-folding, substrate-binding domain

1 | INTRODUCTION

Heat shock proteins are critical components of in vivo defence mechanisms against physical and chemical stresses. Hsp70, a universal and highly conserved 70-kDa heat shock protein, is the central hub of this protein quality control network. Structural studies demonstrate that Hsp70 is comprised of two domains: a 45kDa N-terminal nucleotide-binding domain (NBD) and a 25 kDa C-terminal substrate-binding domain (SBD) (Bertelsen et al., 1999; Flaherty et al., 1990; Zhu et al., 1996). The NBD consists of two α-helix-rich lobes with a deep ATP-binding cleft between them and confers ATP hydrolysis activity to Hsp70s (Flaherty et al., 1990). The

SBD consists of a β-sheet-rich substrate-binding site (SBDβ), a flexible α-helical lid domain (SBDα) that restricts access to the cavity by docking onto SBDβ (Gong et al., 2018; Zhu et al., 1996), and a C-terminal unstructured tail region mediating substrate capture (Bertelsen et al., 1999; Gong et al., 2018). NMR studies suggest that after ADP binding the NBD and SBD connect only through a flexible linker region and without any other intimate contacts (Bertelsen et al., 2009). In contrast, ATP binding leads to a rearrangement of the entire structure and formation of an interface between the NBD and SBD that results in decreased substrate-binding affinity of the SBD (Mayer & Gierasch, 2019; Mayer et al., 2000). The docking of the SBD onto the NBD not only opens up the substrate-binding site of

the SBD, but also locks the rotation of NBD lobes and compromises ATP hydrolysis (Mayer & Gierasch, 2019). It is, thus, proposed that there is a bidirectional allosteric intra-molecular regulation between the NBD and SBD.

Hsp70 is able to interact with hydrophobic stretches of proteins to assist protein folding and refolding, and thus protects cells from a variety of stresses (Mayer & Gierasch, 2019; Tyedmers et al., 2010). A recent study highlighted the versatility of the DnaK (*E. coli* Hsp70) protein, through the identification of approximately 700 substrates (Calloni et al., 2012). This versatility depends on: (1) a tweezers-like functioning of the SBD, which interacts with broad degenerate sequence motifs; (2) substrate interactions that are mediated by a complex allosteric mechanism that coordinates ATP hydrolysis of the NBD; (3) J-domain proteins (such as Hsp40, Ydj1) and NEFs (nucleotide exchange factors) that regulate the allosteric mechanism of Hsp70 (Mayer & Gierasch, 2019). Deciphering the allosteric mechanism behind substrate-binding in the SBD is a key component in understanding the versatility of Hsp70 chaperone function.

Hsp70 proteins are highly conserved across species. *Saccharomyces cerevisiae* is a well-established model for studying Hsp70, with the major cytosolic activity provided by the Hsp70-Ssa family (Ssa-**S**tress **S**eventy subfamily **A**). The Hsp70-Ssa family consists of four members (Ssa1-4) (Lotz et al., 2019). Ssa1-2 are constitutively expressed, with Ssa1 upregulated on exposure to stress, while Ssa3 and 4 are only expressed under stress conditions (Verghese et al., 2012). In addition to their role in responding to stress, the Hsp70-Ssa family are important regulators in the propagation of the yeast [*PSI*⁺] prion. [*PSI*⁺] is the prion form of the Sup35 protein, a translation termination factor that has been extensively studied in relation to the influence of chaperones on its occurrence and propagation (Jones & Masison, 2003; Jones et al., 2004; Jung et al., 2000; Wickner & Masison, 1996). Since the discovery of prions in yeast (Wickner, 1994) protein chaperones have been identified as key modulators of prion propagation (Jones & Tuite, 2005). Hsp104 was the first identified protein shown be essential to maintain propagation of [*PSI*⁺] (Chernoff et al., 1995). The Hsp70 chaperone machinery, including Hsp40s, has since been characterized as working in combination with Hsp104 to maintain prion seed availability for transmission to daughter cells and also maintaining the size of prion aggregates in vivo (Matveenko et al., 2018). Additional flexibility in prion propagation and in maintaining the heat shock response is achieved through functional differences within the highly homologous Hsp70-Ssa family (Lotz et al., 2019; Masison et al., 2009; Xu et al., 2018). As well as assessing factors that influence prion propagation, yeast is also well-established as a model organism for studying protein misfolding diseases such as Huntington's, Alzheimer's and Parkinson's, with genetic screens proving highly valuable for identifying novel cellular factors influencing these diseases (Panaretou & Jones, 2014).

Genetic and biochemical studies in yeast have identified many mutations of Hsp70 (Ssa1) that have the ability to impair propagation of yeast prions and/or influence cell growth, with the majority being located in the ATPase domain (Jones & Masison, 2003; Loovers et al., 2007). L483W was the first mutant located within the SBD to be well-characterized that impairs prion propagation and the heat shock response (Jung et al., 2000; Xu et al., 2017). Recently, residue L484 in the SBD of DnaK (homologous to L483 in yeast Ssa1) has been shown to play a critical role in the regulation of signal transduction from the SBD to the NBD (Kityk et al., 2015). Similarly, we identified another SBD variant, F475S, which mediates [*PSI*⁺] propagation and the heat-shock response in a similar, but more dramatic way as L483W (Xu et al., 2017). F475S and L483W are located in β6 and β7 regions respectively in the SBD. Considering they are close neighbors within the 3D structure of the SBD, we proposed that the β6/β7 region of the Hsp70 substrate-binding domain is a key mediator of the heat-shock response and prion propagation in vivo (Xu et al., 2017).

Here, we further investigate the key role of the β6/β7 region of the SBD domain of Hsp70 in determining functionality. We assess the in vivo structural and molecular characteristics of the β6/β7 region of SBD through targeted mutational analysis of F475 and L483. We found that the size of the hydrophobic side chain on residue 475 is the key factor in determining structural integrity of the β6/β7 region. Interestingly, we identified the vacuolar carboxypeptidase (Pep4) as the possible route for Hsp70-Ssa protein cleavage/degradation rather than the proteasome. Our results confirm our previous finding that mutations at F475 and L483 cause changes to ATPase and protein folding abilities that ultimately compromise the stress response and prion propagation. Our findings suggest that the β6/β7 region is a key mediator, and perhaps the central hub, for determining structural integrity and functionality of the Hsp70 SBD and identify this region of the protein, either directly or indirectly, as a possible druggable target.

2 | MATERIALS AND METHODS

2.1 | Plasmids and yeast strains

The *SSA1* gene and desired mutations were constructed in pC210 plasmid (*SSA1* under own promoter with *LEU2* marker) (Sondheimer et al., 2001; Xu et al., 2013, 2017). Plasmids were transformed into strain G402 (*MAT*a *ade2-1 SUQ5 kar1-1 his3 leu2 lys2 trp1 ura3 ssa1:: KanMX, ssa2::HIS3, ssa3::TRP1, ssa4::ura3-1f/pRDW10*) (Mandal et al., 2017), and cells that had retained the pRDW10 (*SSA1* under own promoter) *URA3* plasmid containing wild-type Ssa1were selected against by re-streaking transformed cells onto plates containing 5-fluoroorotic acid (5-FOA). The *ade2-1* allele is a nonsense mutation in the *ADE2* gene that causes the build-up of red pigment in yeast colonies. The presence of the yeast prion [*PSI*⁺] results in reduced levels of translation termination at nonsense mutations and there for causes a high level of readthrough of *ade2-1*. The result is functional Ade2 protein and no build-up of the red pigment. Hence, [*PSI*⁺] colonies appear white on complete medium with limiting adenine and can grow on medium lacking adenine, while [*psi*⁻] cells are red and require adenine supplementation to grow.

2.2 | Yeast growth assay

Yeast strains were cultured in 5 ml YPD or SC with appropriate selection at 30°C overnight. The following morning, the yeast cultures were diluted to an OD$_{600}$ of 0.2, and grown until the OD$_{600}$ reached 0.5. A 1/5 serial dilution was performed in a 96-well plate and then replicated onto appropriate media. Plates were incubated at 30°C or elevated temperatures (37°C or 39°C) for 2 days as required.

2.3 | Protein purification

Full-length Ssa1 (residues 2-642), truncated Ssa1 (residues 382–554) and corresponding mutations were purified as previously described (Xu et al., 2017). Briefly, full-length Ssa1 and mutations were firstly purified on a Ni affinity column (GE Healthcare) in 50 mM Tris buffer (pH 7.5), 300 mM NaCl and 3 mM β-mercaptoethanol. Following Ulp1 cleavage to remove the N-terminal His-Smt3 tag and a second Ni affinity column purification, the flow through including tag-free protein was further purified by gel filtration chromatography (Superdex 200, GE Healthcare) in 50 mM Tris buffer (pH 7.5), 100 mM KCl, and 5 mM MgCl$_2$. The truncation mutants were similarly purified with some modifications to buffers. For Ni affinity purification, 50 mM Tris buffer (pH 8.0) and 200 mM NaCl was used. Gel filtration chromatography was performed in 50 mM Na-phosphate buffer (pH 7.0) with 50 mM NaCl (Superdex 75, GE Healthcare).

2.4 | Circular dichroism spectroscopy

The CD spectra of full-length Ssa1 and mutations were obtained in 50 mM Tris buffer (pH 7.5), 100 mM KCl and 5 mM MgCl$_2$ at a protein concentration of 3 μM using a Chirascan Plus CD spectrometer (Applied Photophysics, UK). Spectra were measured from 200 to 260 nm in a 10 mm path-length thermostat-controlled quartz cuvette. The temperature was controlled using a Peltier device. The truncation mutants, at a protein concentration of 10 μM, were measured in 50 mM Na-phosphate buffer (pH 7.0) with 50 mM NaCl.

2.5 | Size exclusion chromatography

Recombinant proteins were incubated at RT for 0 hr or 24 hr. The pattern and degradation of SBD truncation mutants were evaluated by Size exclusion chromatography (SEC) (Superdex 75, 24 ml GE Healthcare) in 50 mM Na-phosphate buffer (pH 7.0) with 50 mM NaCl at RT.

2.6 | ATPase assay

The ATPase activity was measured based on colorimetric determination of inorganic Na-phosphate using malachite green as previous described (Rowlands et al., 2004; Xu et al., 2017). Briefly, 10 μl of 2 μM Ssa1 (50 mM Tris pH 7.5, 100 mM KCl, 5 mM MgCl$_2$, and 1 mM DTT) was added with 10 μl of 2 mM ATP into each well of a 96-well plate, and then incubated for 5 hr at the indicated temperature. If Ydj1 or peptide (ALLLSAPRR) was required, a final concentration of 8 μM or 400 μM was used, respectively.

2.7 | Luciferase refolding assay

The luciferase assay was carried out as previously described (Xu et al., 2017). Briefly, overnight cultures were diluted to an OD$_{600}$ of 0.2 in SC media without uracil (SC-URA) and incubated at 37 °C with shaking for 30 min to induce expression of heat shock proteins. After culturing, the cellular luciferase activity of each strain was measured by immediately adding 10 μl of decanal (Sigma) to 200 μl of culture in a FB12 Luminometer (Berthold Detection Systems) as a reading for 100% activity. Cells were then transferred into a 45°C shaking incubator for 1 hr. During this 1 hr heat shock, cycloheximide (Sigma) was added after 50 min at 10 μg/ml. After thermal denaturation at 45°C, cellular luciferase activity was measured as the starting point ($i = 0$). Cultures were shifted to 25°C at intervals of 15 min for a duration of 1 hr. The luciferase recovery ratio was calculated based on the starting point ($t = 0$) and ending point after 1 hr recovery as a percentage of the 100% activity.

2.8 | Protein extraction from yeast

Yeast strains were cultured overnight in 5 ml YPD or selective media at 30°C. The following morning, cells were diluted in 25 ml fresh same media to an OD$_{600}$ of 0.2 and incubated until an OD$_{600}$ of 0.6–0.8 was reached. Washed cell pellets were resuspended in yeast cell lysis reagent (Sigma C4482) complemented with 10 mM DTT and protease inhibitor cocktail (Sigma P8215). Glass beads of 0.5 mm were used to aid cell lysis using a MiniBeadbeater (Biospec products). For inhibitor treatments, the fresh WT/F475S cells were cultured at 30°C in SC containing 0.1% (w/v) L-Proline to OD$_{600}$ 0.5, then cells were harvested and resuspended in 20 ml of fresh SC with 0.003% (w/v) SDS containing 75 μM MG132 or 1 mM PMSF for another 2 hr incubation at 30°C before harvesting and homogenization.

2.9 | Immunoprecipitation

Anti-Flag M2 Magnetic Beads (Sigma) were used to purify Flag-tagged Ssa1 in yeast cells. A 300 μg sample of protein was extracted and incubated with 20 μl Magnetic Beads with gentle rotation at 4°C overnight. Magnetic Beads were collected using a magnetic separator and washed with 10 volumes of TBS (50 mM Tris-HCl, 150 mM NaCl, pH 7.5) four times followed by the addition of three volumes of 3 × Flag peptide of 150 ng/μl and incubation on a rotator for 1 hr at 4°C. Supernatants were transferred to pre-chilled 1.5 ml microfuge

tubes and centrifuged (10 min, 13,000 rpm). Then 25 µl was analyzed by Western blotting.

2.10 | Cleavage assay

For SBD cleavage assay under heat shock or AZC treatments, G402 strains were cultured in 6 ml YPD media overnight at 30 °C with shaking. The following morning, part of the overnight cultures were diluted in 25 ml SC containing 300 µg/ml AZC to an OD_{600} of 0.2. For the heat shock treatment, overnight cultures were diluted in 25 ml YPD media to an OD_{600} of 0.2. When an OD_{600} of 0.5 was reached, untreated and AZC treated cells were kept at 30°C and the other cells were heat shocked at 39°C (2 hr or 3 hr). Protein extraction, immunoprecipitation and Western blot were performed to investigate the cleavage of Ssa1 and its mutations.

2.11 | Molecular dynamics simulation

Molecular dynamics (MD) simulations were performed using the GROMACS 4.5.7 and 4.6 package (Van Der Spoel et al., 2005) as described previously (Xu et al., 2013). The homologous Hsp70 solution structure of Ssa1, DnaK SBD with peptide NRLLTG (PDB code: 1Q5L) (Stevens et al., 2003) was used as wild type. Appropriate mutants were constructed using Swiss-Pdb Viewer (Guex & Peitsch, 1997) based on wild type. Simulations were carried out over a 20 ns period at 300 K, pH 7.0, and 1 bar pressure. The coordinate trajectories were saved for subsequent data analysis.

2.12 | Statistical analysis

Student's t-test was used, where appropriate, for statistical analysis. Sample sizes used were in line with other similar published studies. Data are presented as mean ± SD. Statistical analysis was performed using the statistical software package GraphPad Prism v6 or Microsoft EXCEL. $p \leq .05$ was considered statistically significant.

3 | RESULTS

3.1 | Evolutionarily conserved F475 mediates function in the Hsp70-Ssa family

The F475S variant of Ssa1 has been characterized as impairing both the heat shock response and [PSI⁺] propagation (Xu et al., 2017). However, whether this is the case for the whole Hsp70-Ssa family has not been determined. F475 is highly conserved among the Hsp70 family of proteins, not only in yeast, but also in human and E. coli homologues (Figure 1a). F475 is found to be the most conserved

residue situated in β6 and is proximal to the hydrophobic core of the SBD (Figure 1a,b).

To further investigate the role of F475 in the Ssa subfamily, the F475S mutation was introduced into Ssa2-Ssa4, and phenotypically assessed with these mutants providing the sole source of cytosolic Hsp70 in vivo. Similar to Ssa1^F475S, Ssa2^F475S and Ssa4^F475S are unable to propagate [PSI⁺] and are compromised for the heat shock response (Figure 1c,d). Interestingly, Ssa3^F475S is lethal to the cell and further highlights the significance of F475 in maintaining Hsp70 function.

3.2 | F475S destabilizes Ssa1 and results in SBD cleavage and degradation

F475S was proposed to disrupt the hydrophobic core of the SBD and shown to result in degradation in vitro (Xu et al., 2017). To further confirm whether SBD break down occurs in full-length Ssa1, N-terminal Flag-tagged wild-type Ssa1 and its F475S mutant were expressed in G402 cells as the sole source of cytosolic Hsp70, and then enriched by immunoprecipitation. Figure 2a, shows several bands observed around 40–50 kDa in the Flag-F475S sample, which are absent in the wild-type sample. Considering the Flag tag was fused to the N-terminal of Ssa1 and the size of the NBD is around 45 kDa, the cleavage bands of the Flag-F475S suggested that the SBD is readily degraded and results in the production of NBD fragments in vivo or at least in the cell lysate.

Proteins are degraded by two alternative breakdown pathways in S. cerevisiae. Usually, the degradation of short-lived proteins happens in proteasomes and can be inhibited by carbobenzoxyl-leucinyl-leucinyl-leucinal (MG132); vacuolar proteases contribute to degrading long-lived proteins and can be suppressed by phenyl-methylsulfonyl fluoride (PMSF) (Lee & Goldberg, 1996). To distinguish between the cytosolic versus vacuolar proteolytic pathway contribution to SBD cleavage/degradation, we added each class of inhibitor separately into cultures to prevent protein degradation. Western blotting showed that the basal Ssa1 level of F475S was comparable with DMSO treatment after MG132 inhibitor incubation but enhanced after treatment with PMSF (Figure 2b), suggesting SBD cleavage/degradation mainly occurred by the vacuolar proteinase rather than proteasomal. To confirm this hypothesis, we assessed the SBD cleavage of the F475S variant in three knockout strains, ΔPEP4 (vacuolar carboxypeptidase deficient), ΔUFD2 (ubiquitin fusion degradation factor deficient) and ΔUBI4 (ubiquitin precursor deficient) by transforming the Flag-tagged F475S variant into each of these three backgrounds. Cells were then cultured in SC-Leu, and Flag-Ssa1 was enriched using anti-Flag beads. As shown in Figure 2c, the abundance of full-length F475S variant was significantly increased in ΔPEP4 with corresponding reduced levels of cleavage products. Both ΔUFD2 and ΔUBI4 do not significantly reverse the cleavage pattern. This result clearly shows that the major proteolysis for Hsp70 cleavage due to F475S structural perturbation, may be through a Pep4 [vacuolar carboxypeptidase]-dependent mechanism.

(a)

(b)

(c)

(d)
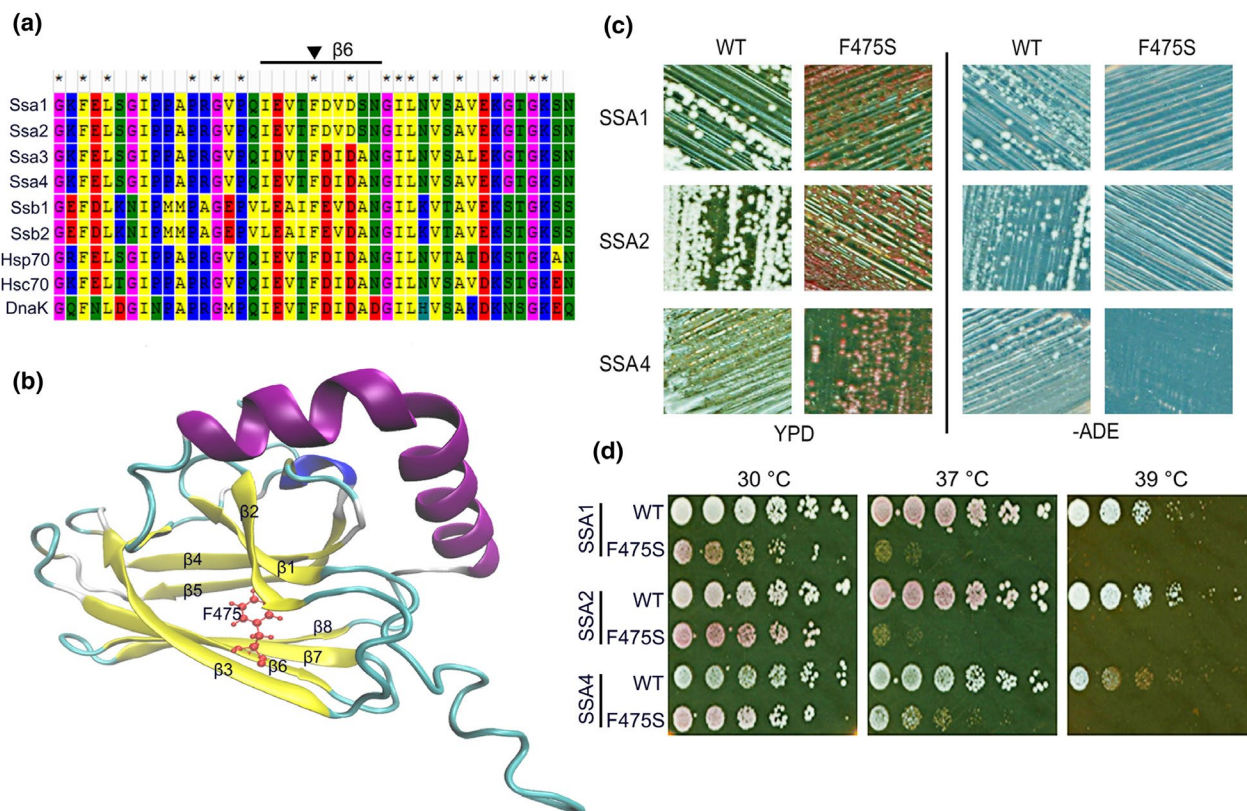
FIGURE 1 Evolutionarily conserved residue 475 mediates cellular functions of Hsp70. (a) Alignment of Hsp70 proteins from yeast, human and *E. coli*. (b) The residue Phe475 is adjacent to the substrate-binding pocket on Ssa1. Phe475 is shown in red on the Ssa1 structure (PDB: 5Z8I). (c) [*PSI*⁺] prion propagation in Ssa mutants. A single colony with sole Ssa source containing homologue F475S variant was streaked onto YPD and -ADE plates and grown for 2 days at 30°C. [*psi*⁻] cells produce red colonies on YPD and do not grow on -ADE plates. [*PSI*⁺] cells produce white colonies on YPD and grow on -ADE plates. (d) Temperature sensitivity of Ssa mutants. Cells expressing WT Ssa or corresponding F475S homologues as their sole Ssa protein were spotted in a 1/5 serial dilution onto YPD and were incubated for 2 days at 30°C, 37°C or 39°C [Colour figure can be viewed at wileyonlinelibrary.com]

3.3 | Size of the hydrophobic amino acid side chain at residue F475 is the predominant determining factor for impairing Hsp70 function in vivo

To investigate the key molecular factors that determine Hsp70 functional change caused by perturbation of the β6/β7 region, we created a variety of amino acid substitutions at F475 and characterized these genetically and biochemically (Table 1). It was found that hydrophobic residues phenylalanine (F) and tyrosine (Y) maintained Hsp70 cellular functions relating to [*PSI*⁺] propagation and heat-shock response, but hydrophilic serine (S) resulted in severe [*PSI*⁺] impairment and temperature sensitivity (Figure 3a,b,d). The impact of serine at this residue resulted in hydrophobic-core disruption caused by introducing the hydrophilic side chain (Xu et al., 2017). Notably, decreasing the size of hydrophobic side chain of residue 475 to very small alanine (A) resulted in [*PSI*⁺] impairment but very limited temperature sensitivity suggesting the hydrophobic alanine (A) may be too small to fill the hydrophobic cavity around residue 475 (Figure 3a,b,d). Moreover, at the other extreme, the window for increasing the hydrophobic size of the amino acid is also narrow as replacing phenylalanine (F) or tyrosine (Y) with tryptophan (W)

resulted in a non-functional Hsp70 and cell nonviability (Table 1), which may be due to catastrophic disruption of the hydrophobic core (Figure 3a,b,d). Surprisingly, Cysteine (C) substitution compared to serine (S) did not display similar phenotypes, but was more similar to WT (Figure 3a,b,d). This could suggest that Cysteine (C) substitution at F475 influences Ssa1 function through a complicated mechanism rather than disrupting the hydrophobic core only. These phenotypic trends are also observed for other cellular stresses such as cell wall damage (SDS) and oxidative damage (H_2O_2) (Figure 3c). Also, exposure to higher concentrations of oxidative damage revealed a phenotypic difference between F and all other mutations (Figure 3c), which reflects the importance of this highly conserved residue in this region (Figure 1a).

3.4 | The side chain of residue at position 475 is a key mediator of SBD stability

We previously reported that the F475S mutation in Hsp70 results in unfolding of the SBD and accelerates protein degradation (Xu et al., 2017). To evaluate the molecular level changes that induce
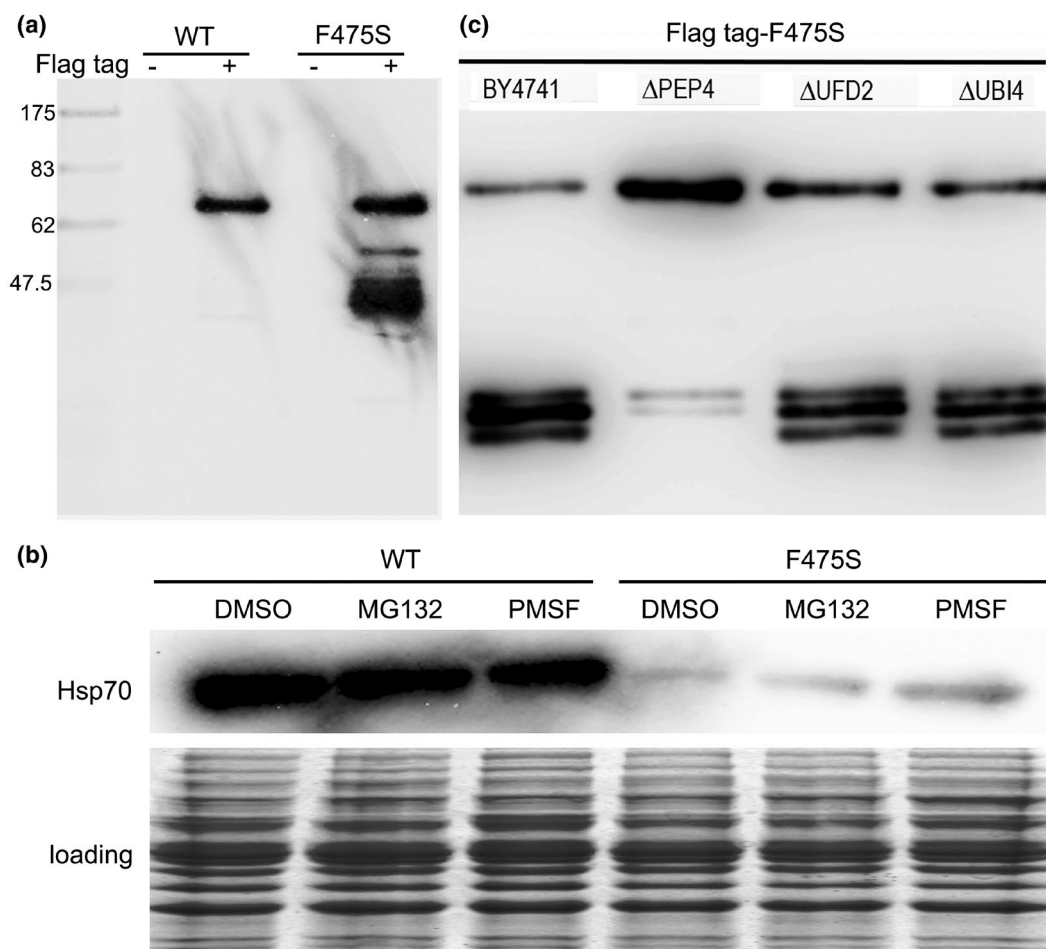
FIGURE 2 Specific SBD cleavage induced by F475S mutation. (a) G402 cells containing N-Flag tagged or tag-free vector were homogenized and precipitated by anti-Flag beads. Anti-Flag was used to probe Flag-tagged Ssa1 proteins and degraded fragments. (b) Effects of degradation inhibitors on the abundance of F475S protein. Western blotting was performed to assess the protein levels of Ssa1 F475S following treatment with MG132 (75 μM) or PMSF (1 mM). DMSO was used to dissolve MG132 and PMSF, and the same volume of DMSO was added as a negative control in cell cultures. A stained SDS-PAGE gel running under the same conditions was used as the loading control. Two independent experiments were performed. (c) Vacuolar carboxypeptidase (Pep4) is primarily responsible for degradation of the SBD. The F475S variant was transformed into ΔPEP4, ΔUFD2 and ΔUBI4 cells. After immunoprecipitation, anti-Flag was used to probe Flag-tagged Ssa1 proteins and degraded fragments

TABLE 1 Amino-acid properties of residue 475

Amino acid at residue 475	Size of the side chain	Polar/nonpolar (+/−)	$[PSI^+]/[psi^-]$	Temperature sensitive
Phe	+	−	+	N
Ser	−−	+	−	Y
Ala	−−−	−	−	Y
Cys	−	+/−	+	N
Trp	+++	−	NA	NA
Tyr	++	−	+	N

SBD unfolding and subsequent degradation, we employed SEC and circular dichroism (CD) to monitor the effects of F475 substitutions on protein conformation and secondary structure. Comparing to standards (Figure S3), Figure 4a demonstrates that F475A, F475C, and F475Y maintain the monomeric state similar to WT, but the lethal mutant F475W had an obvious absorbance shift toward F475S.

As F475S had been confirmed to cause unfolding of the SBD rather than oligomerization (Xu et al., 2017), it was considered that F475W exhibited similar behavior but maybe to a different degree. After a 24 hr incubation at room temperature, there was no aggregated protein observed after centrifugation (13,000 g, 10 min), but we clearly observed a decrease in absorbance at the elution peak and
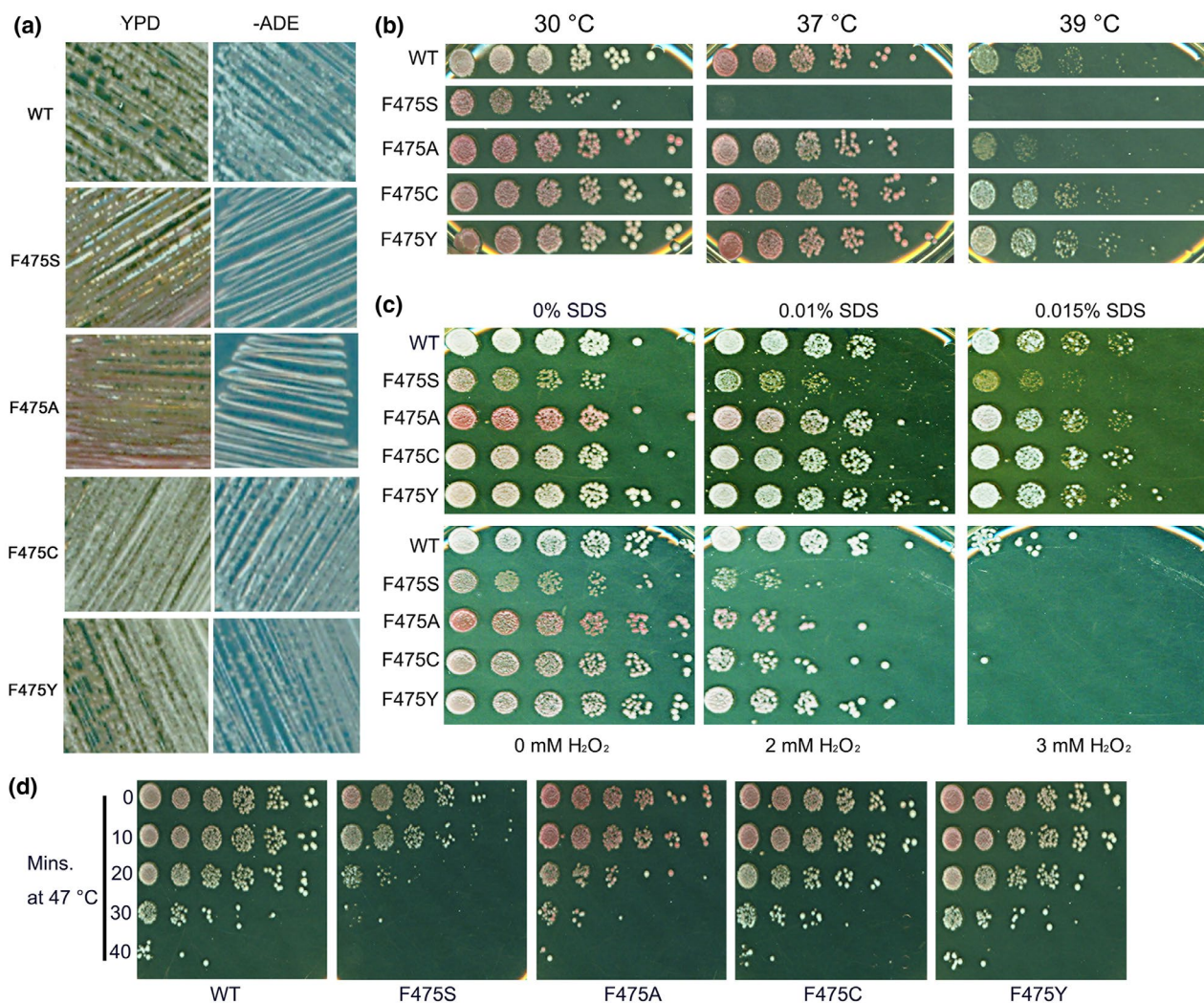
FIGURE 3 Phenotypes of different Phe475 substitutions. (a) Assessments of [*PSI*⁺] propagation; [*psi*⁻] cells produce red colonies on YPD and are unable to grow on -ADE plates; [*PSI*⁺] cells produce white colonies on YPD and grow on -ADE plates. (b) Growth assay of Phe475 mutations at elevated temperatures. Cells expressing WT Ssa1 or corresponding Phe475 mutations as their sole Ssa protein were spotted in a 1/5 serial dilution onto YPD, and were incubated for 2 days at 30°C, 37°C, or 39°C. (c) Growth assay of Phe475 mutations under other stresses. YPD or SC medium was supplemented with cell-wall damage agent SDS or oxidative damage agent H_2O_2 respectively to achieve the required concentrations. (d) Acquired thermotolerance assay of Phe475 mutations. Fresh cultures were pre-treated at 39°C for 1 hr, then cells were heat shocked at 47°C for the indicated times before spotting onto YPD [Colour figure can be viewed at wileyonlinelibrary.com]

a continuous increase in absorbance after the peak, suggesting that both F475S and F475W are less stable and cleaved into smaller fragments in vitro compared with other F475 substitutions (Figure 4b). Consistent with these findings, both F475W and F475S exhibited a disrupted secondary structure in their CD spectra (Figure 4c). Although F475A did not display significant unfolding at 30 °C, we did observe that F475A caused SBD unfolding and reduced stability compared to wild type at elevated temperature (Figure S1), which reflects the milder impairment phenotypic stress response we compared to the S mutation (Figure 3b-d). CD spectra of the full-length Ssa1 proteins shows that F475S and F475W have similar characteristics (Figure 4d). F475S and F475W variants do show a decreased absorbance at 215–217 nm, which reflects loss of β-sheet structure in SBDβ (Figure 4d). Additionally, both mutants caused changes at 208 and 222 nm compared to WT (Figure 4d), which reflects some

conformational change in the α-helical regions in the NBD (Xu et al., 2017).

3.5 | Substitutions at residue 475 alter critical functions of Hsp70

Of critical importance to maintaining Hsp70 functionality is regulation of its ATPase activity. We, therefore, assessed the ATPase hydrolysis activity of each full-length F475 mutant under various conditions. F475S increased the basal ATPase activity, but was incapable of further stimulation by Ydj1, this trend was seen over three temperature ranges (Figure 5a). Notably, heat shock significantly increased the basal ATPase activity of WT, but not F475S (Figure 5a). It has been shown that the SBD acts as a "brake" on the NBD's
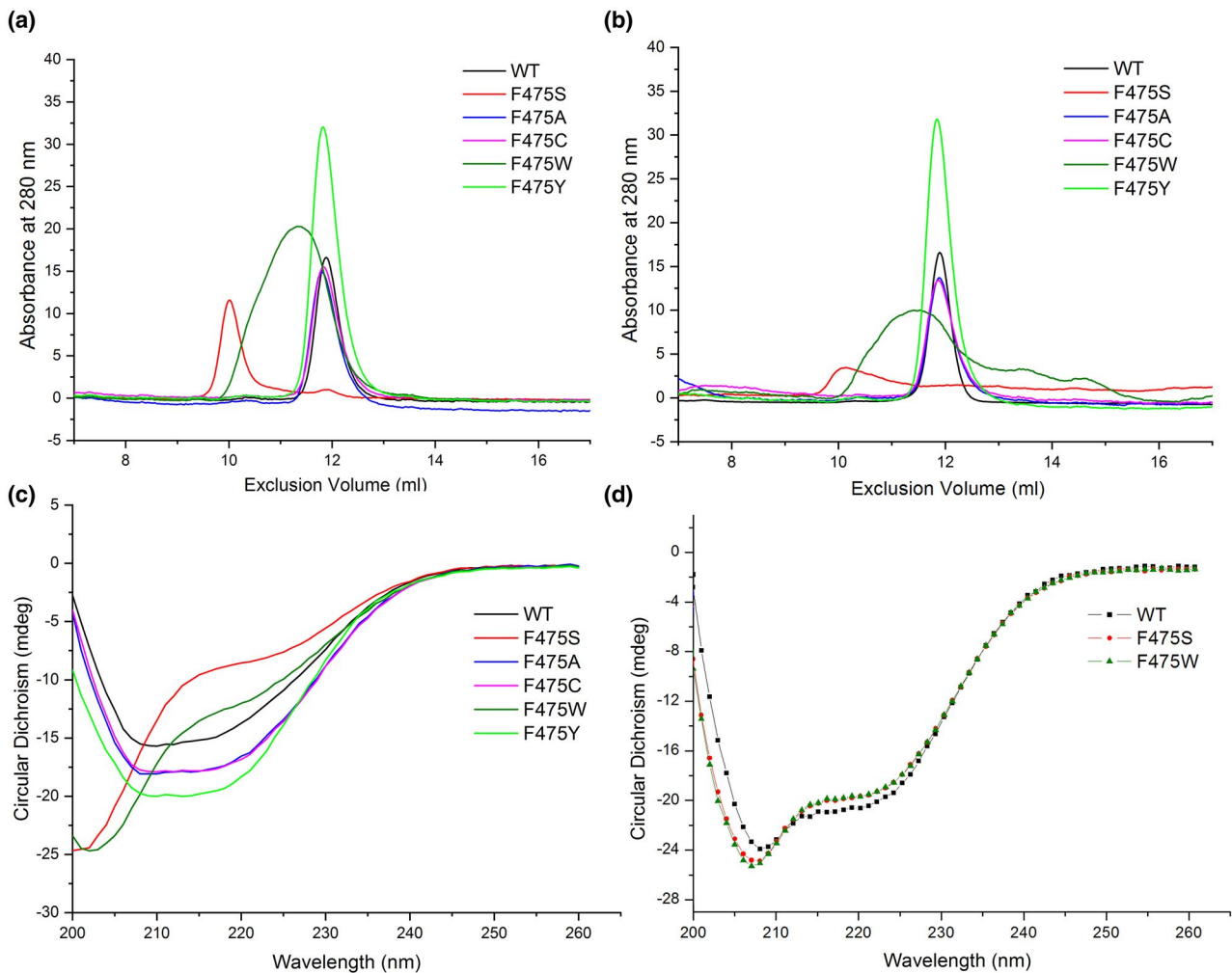
FIGURE 4 Amino acid substitutions at residues 475 alter Hsp70 SBDβ conformation and stability. (a) The elution pattern of SBD truncation proteins. Size exclusion chromatography (SEC) was performed at RT. (b) The stability of SBD truncation proteins. Recombinant proteins were incubated at 30°C for 24 hr and then size exclusion chromatography (SEC) was performed at RT. (c) CD spectroscopy of SBD truncation proteins at 30°C. (d) Secondary structure monitored by far-UV CD spectra for full-length Ssa1 at 30°C [Colour figure can be viewed at wileyonlinelibrary.com]

ATPase activity and that the free NBD with the linker domain attached has a higher ATPase activity than full-length Hsp70 (O'Brien & McKay, 1993). Thus, one possible reason for enhanced ATPase activity is that heat shock causes perturbation of the SBD which leads to a reduction in SBD-mediated repression of ATPase activity of the NBD. To investigate whether SBD cleavage occurred after heat shock, we enriched flag-tagged Ssa1 from cell lysate to minimize protein-level influence caused by heat shock and detected Ssa1 fragments as Figure 2a. Interestingly, degraded fragments of Hsp70 of approximately 45 kDa can be observed from cells exposed to heat shock, suggesting SBD undergoes cleavage under these conditions in vivo or at least in cell lysis (Figure 5d, left panel). Additionally, this observation was confirmed using a heat-shock mimetic compound azacytidine (AZC) (Figure 5d, right panel). Similar to F475S (Xu et al., 2017), F475W significantly increased ATPase activity at 30 °C (Figure 5b). In contrast, F475A has a small effect on basal ATPase activity and F475C/Y are similar to WT (Figure 5b). Notably, the ATPase activity of F475W is also not stimulated by Ydj1 (Figure 5b).

Additionally, F475S/W, but not F475A/C/Y, showed compromised ATP hydrolysis stimulated by peptide binding (Figure 5c). The elevated basal ATPase rate by SBD mutants (especially F475W and F475S) and compromised ATP stimulation by client binding implies that SBD disruption abolishes the inhibition of ATP hydrolysis of NBD.

The Hsp70/Hsp40/Hsp104 machinery plays an essential role in protein folding and the heat-shock response. Previously we demonstrated that F475S is deficient in luciferase refolding (Xu et al., 2017). Unsurprisingly, the F475A mutation, which also exhibits a [psi⁻] phenotype, had reduced ability to refold denatured luciferase, and F475C/Y displayed a comparable refolding activity with WT (Figure 6a). Additionally, we assessed the abundance of selected chaperones and found that Hsp104 and Ydj1 were expressed at similar levels in WT and all mutants. However, we observed a variant pattern in abundance of Ssa1 within the mutants. Surprisingly, F475C, which had no dramatic phenotypic effects, exhibited greatly reduced levels of Ssa1 that were similar to F475S (Figure 6b), while
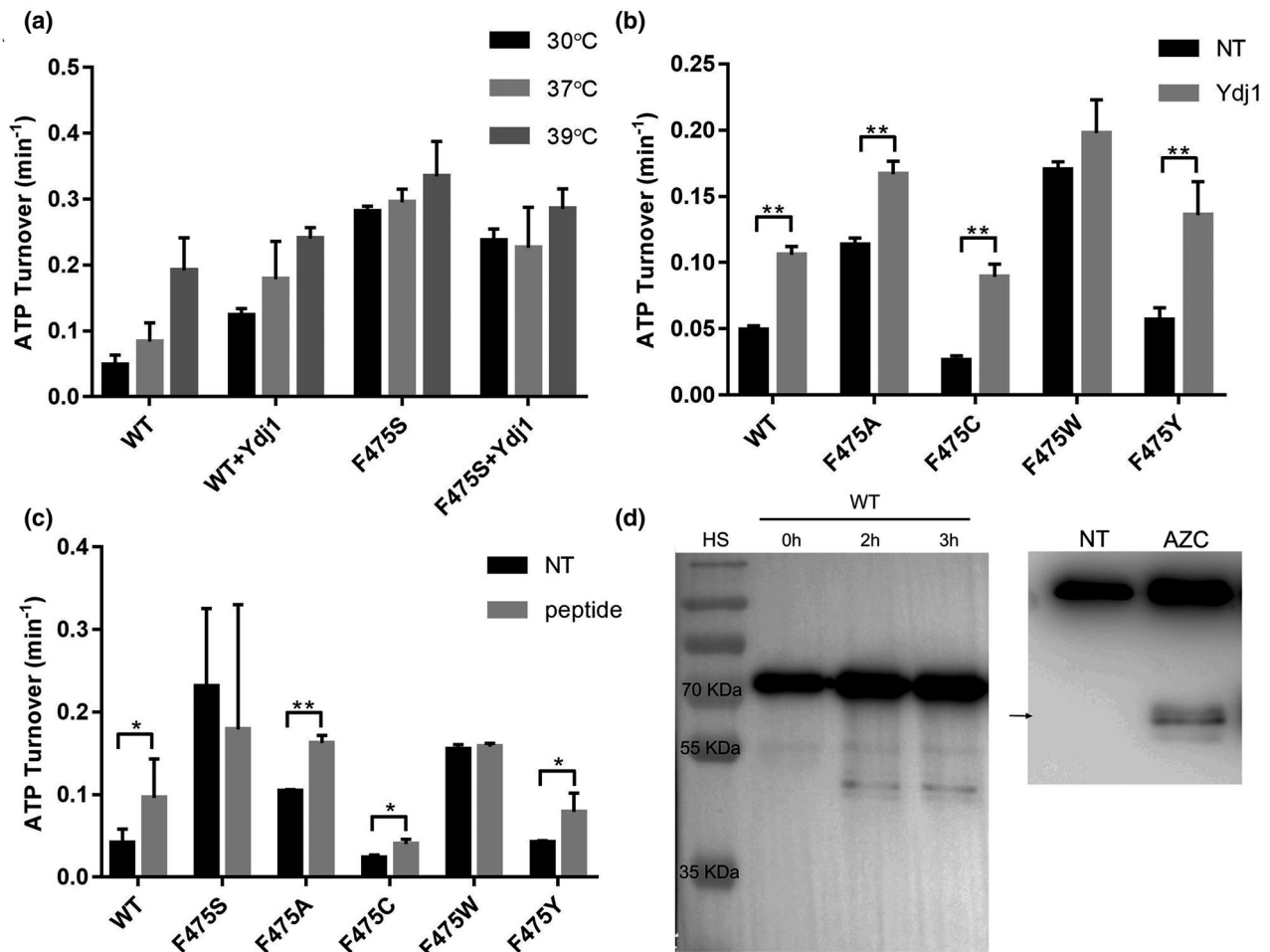
FIGURE 5 Variants at residue 475 alter ATPase activity of Ssa1. (a) The ATPase activity of the full-length Ssa1 proteins. ATPase assay was performed at 30°C, 37°C, or 39°C. (b) ATPase activity stimulated by Ydj1. (c) ATPase activity stimulated by addition of peptide. The unit of the ATP turnover rate is min^{-1}. The values shown are the mean of four or eight replicates from independent measurements and the error bars represent the standard deviation. (d) Specific SBD cleavage during heat shock. WT cells were grown at 39°C for times as indicated (left panel) or cultured in SC containing 300 µg/ml AZC for 2 hr (right panel). After Flag-Ssa1 precipitation, Anti-Flag was used to probe Flag-tagged Ssa1 proteins

F475A, which exhibits the most similar phenotypic profile to F475S, in contrast to this mutant, expressed high levels of Ssa1 (Figure 6b).

3.6 | Substitutions at residue 483 alter critical functions of Ssa1

In addition to F475, L483 also located in the β6/β7 region has been reported and characterized as impairing [*PSI*⁺] propagation (Xu et al., 2013, 2017). Furthermore, using steered molecular dynamics simulations, it is possible to predict prion propagation phenotypes when introducing mutations at L483 (Xu et al., 2013). We find that amino acids with a large side chain (L483W/H) at this residue not only impaired [*PSI*⁺] propagation (Xu et al., 2013), but also compromise thermotolerance (Figure 7a). Similar to F475S, both L483W and L483H display a deficiency in luciferase refolding activity (Figure 7b), each have elevated basal ATPase activity and compromise stimulation by Ydj1 and peptide (Figure 7c). Additionally, there

are no significant differences in Hsp104 and Ydj1 expression, but decreased Ssa1 abundance is observed for L483W and particularly for L483H (Figure 7d).

3.7 | Substitutions at residue 483 alter stability of the SBD

We evaluated the influence of substitution mutations at residue 483 upon conformation and stability, by obtaining CD spectra of purified SBD mutants. L483W/H exhibited decreased absorbance at 215–217 nm compared to WT, which implies a loss of β-sheet structure in the SBDβ (Figure 8a), although not to the same extent as F475S/W (Figure 4c). Additionally, compromised β-sheet content can be observed from full-length proteins for L483W/H and both mutants have reduced absorbance at 208 and 222 nm suggesting a structural change within the NBD also (Figure 8b) (Xu et al., 2017), which may explain the enhanced ATPase of L483W/H
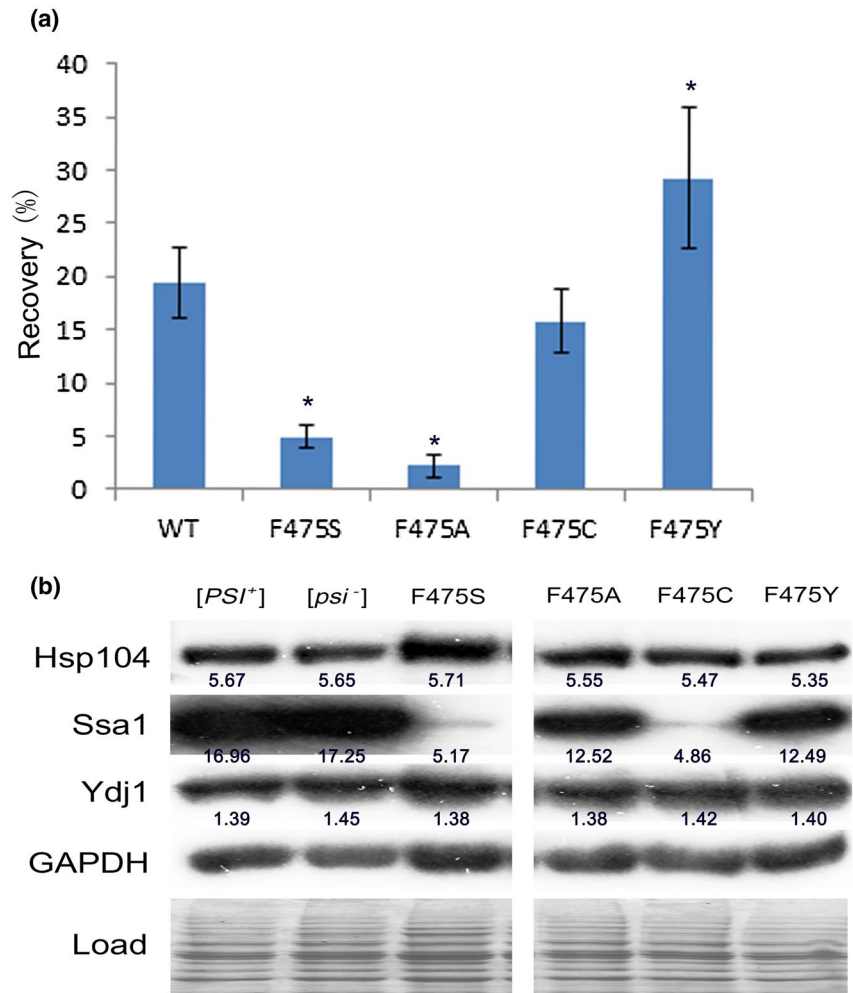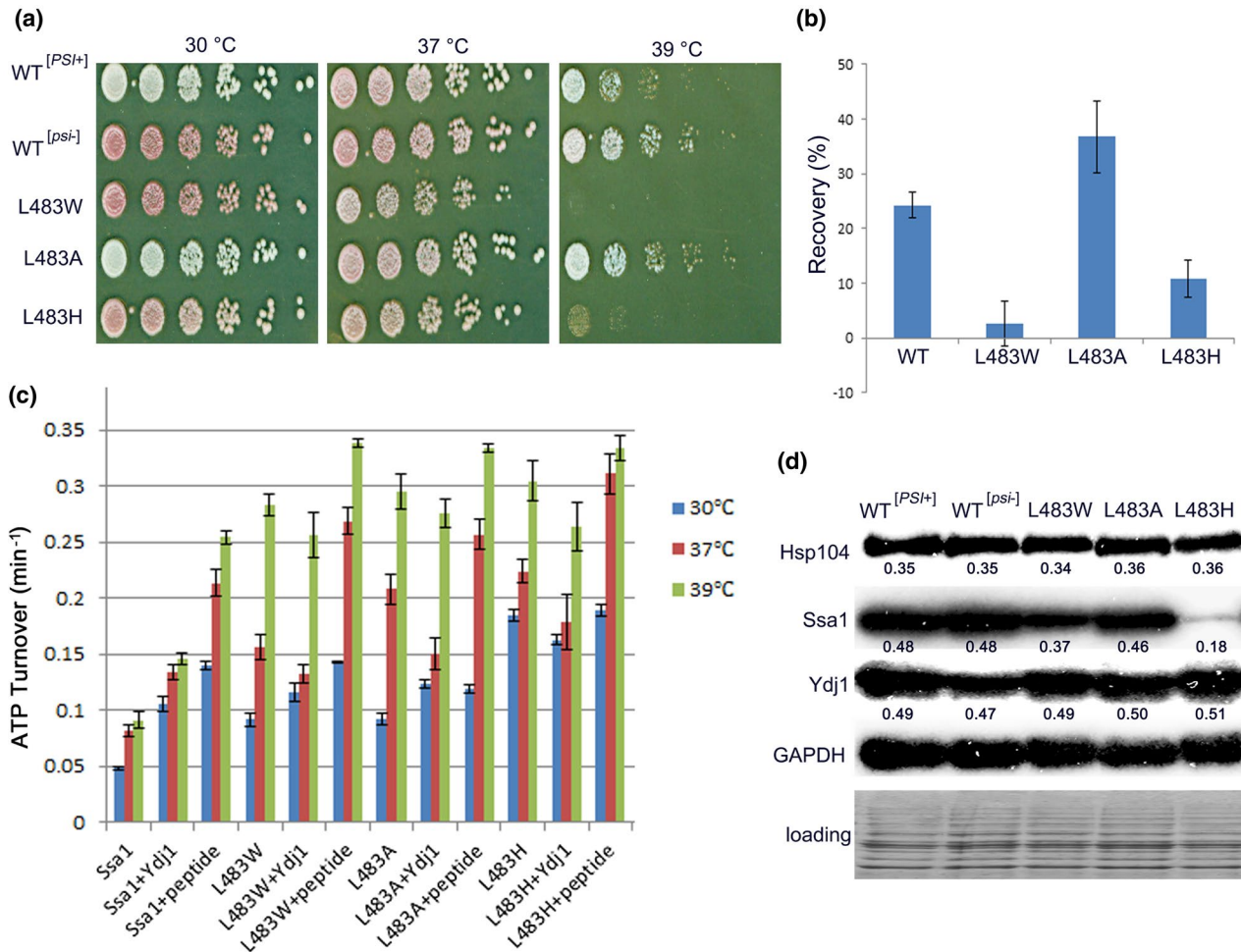
FIGURE 6 Variants at residue 475 alter functions of Ssa1. (a) Luciferase refolding activity of Phe475 mutations in vivo. Fresh cultures were shifted to 37°C for 30 min before 45°C denaturation for 1 hr. Denatured luciferase cultures were recovered at 25°C for a 1 hr period. Cycloheximide was added to prevent protein synthesis during the recovery period. (b) Chaperone abundance of the Hsp70 machinery. Western blotting was performed to assess the abundance of Hsp104, Ssa1, and Ydj1. GAPDH and a stained SDS-PAGE ran under the same conditions were used as loading controls. Protein content was normalized to GAPDH (protein/GAPDH ratio) [Colour figure can be viewed at wileyonlinelibrary. com]

variants. Molecular simulations were employed to assess what may happen once the large side chain was introduced at residue 483. Simulations predict that the larger side chain of W and H, compared to L or A, could easily perturb the microenvironment by infiltrating the hydrophobic core (Figure 8c,d). As a consequence, the SBD of L483W/H may induce the same mechanism that unfolds the SBD and results in an instability profile similar to the F475S/W mutants (Figures S2, 4a-c, and 8a). In particular L483H, exhibits severe thermotolerance phenotype and has the most extreme effects on abundance and predicted structural perturbation (Figures 7a,d, 8a, and S2).

4 | DISCUSSION

The essential role Hsp70 plays in protein folding and in survival following exposure to a variety of stresses, has been demonstrated in a number of species (Abravaya et al., 1992; Bettencourt et al., 1999; Morimoto & Santoro, 1998; Xu et al., 2019). The key to Hsp70 functionality is the coordination and communication between the NBD and SBD (Mayer & Gierasch, 2019). Recent studies have identified amino acid residues in the SBD that play critical

roles in signal transduction to the NBD (Kityk et al., 2015) and highlight the β6/β7 region as an important mediator of peptide binding and structural stability (Xu et al., 2017). Within the β6/β7 region the two highly conserved residues are F475 and L483 (residue numbers from yeast Ssa1 protein) (Figure 1a). The importance of these residues has been isolated in studies using yeast, when mutants of both residues, namely F475S and L483W, have been isolated from genetic screens that identified Hsp70 mutants that impaired prion propagation (Jung et al., 2000; Xu et al., 2017). The F475S mutation has the most extreme effects on in vivo function in that yeast cells expressing this variant as the sole source of Hsp70-Ssa are unable to propagate the prion state [PSI+] and are unable to tolerate a variety of stresses (Xu et al., 2017). The main goals of this study were to assess the in vivo consequences of F475S across the Hsp70-Ssa family and to identify the molecular level changes that occur in mutants created at residues 475 and 483, and correlate molecular changes with phenotypic outcome. To assess if the phenotypic effects of F475S are replicated in the Hsp70-Ssa family, we created isogenic yeast strains expressing Ssa1, 2, 3, or 4 variants of F475S as the sole source of cytosolic Hsp70. Given the high degree of sequence identity between members of the Ssa family, it is not surprising that the F475S mutation has major

FIGURE 7 Substitutions of residue 483 alter molecular and cellular functions of Ssa1. (a) Growth assay of Leu483 mutations at elevated temperatures. Cells expressing WT Ssa1 or corresponding Leu483 mutations as their sole Ssa protein were spotted in a 1/5 serial dilution onto YPD and then incubated for 2 days at 30°C, 37°C, or 39°C. (b) Luciferase refolding activity of Leu483 mutant yeast strains. Fresh cultures were shifted to 37°C for 30 min before 45°C denaturation for 1 hr. Denatured luciferase cultures were allowed to recover at 25°C for a 1 hr period. Cycloheximide was added to prevent protein synthesis during the recovery period. (c) The ATPase activity of the full-length Ssa1 proteins. ATPase assay was performed at 30°C, 37°C, or 39°C with stimulation by Ydj1 or peptide. The unit of the ATP turnover rate is min^{-1}. The values shown are the mean of four replicates from independent measurements and the error bars represent the standard deviation. (d) Chaperone abundance of the Hsp70 machinery. Western blotting was performed to assess the expression levels of Hsp104, Ssa1, and Ydj1. GAPDH and a stained SDS-PAGE run under the same conditions were used as loading controls. Protein content was normalized to GAPDH (protein/GAPDH ratio) [Colour figure can be viewed at wileyonlinelibrary.com]

phenotypic effects on all these strains. Ssa1, 2 and 4 proteins harboring F475S have similar prion propagation and thermotolerance phenotypes (Figure 1c,d), while Ssa3^{F475S} cannot maintain cell viability. Presumably Ssa3 is more susceptible than other Ssa proteins to the structural perturbations caused by F475S and hence is degraded more rapidly. While the Ssa family are highly conserved and do exhibit redundant functionality at times, there are many studies that highlight functional differences between family members and in particular Ssa3, a recent example being the identified link between autophagy and Ssa3 (Gupta et al., 2018). It is clear that similar to L483W, which has been shown to exhibit prion impairing effects in different Ssa isoforms (Loovers et al., 2007; Sharma & Masison, 2008), F475S causes severe loss of function across the whole Hsp70-Ssa family.

Our previous study identified instability of the SBD and unfolding of the β6/β7 region as the primary initiating event and the cause of Hsp70-Ssa1 loss of function due to F475S (Xu et al., 2017). To investigate further the molecular level events that occur in the β6/β7 region that lead to functional change in Hsp70, we created a range of amino acid substitution mutations at both 475 and 483, and assayed for functional change through a range of genetic, biochemical and structural techniques. The major finding from this analysis is that the key factor to maintaining or perturbing the structural integrity of the SBD, is the size of the hydrophobic amino acid occupying these two key residue sites. The introduction of hydrophilic Ser or extremely small hydrophobic Ala at 475 causes the greatest phenotypic changes and results in loss of [*PSI*$^+$] propagation and reduced stress tolerance (Figure 3a–d). This is because when the extremes of the tolerance
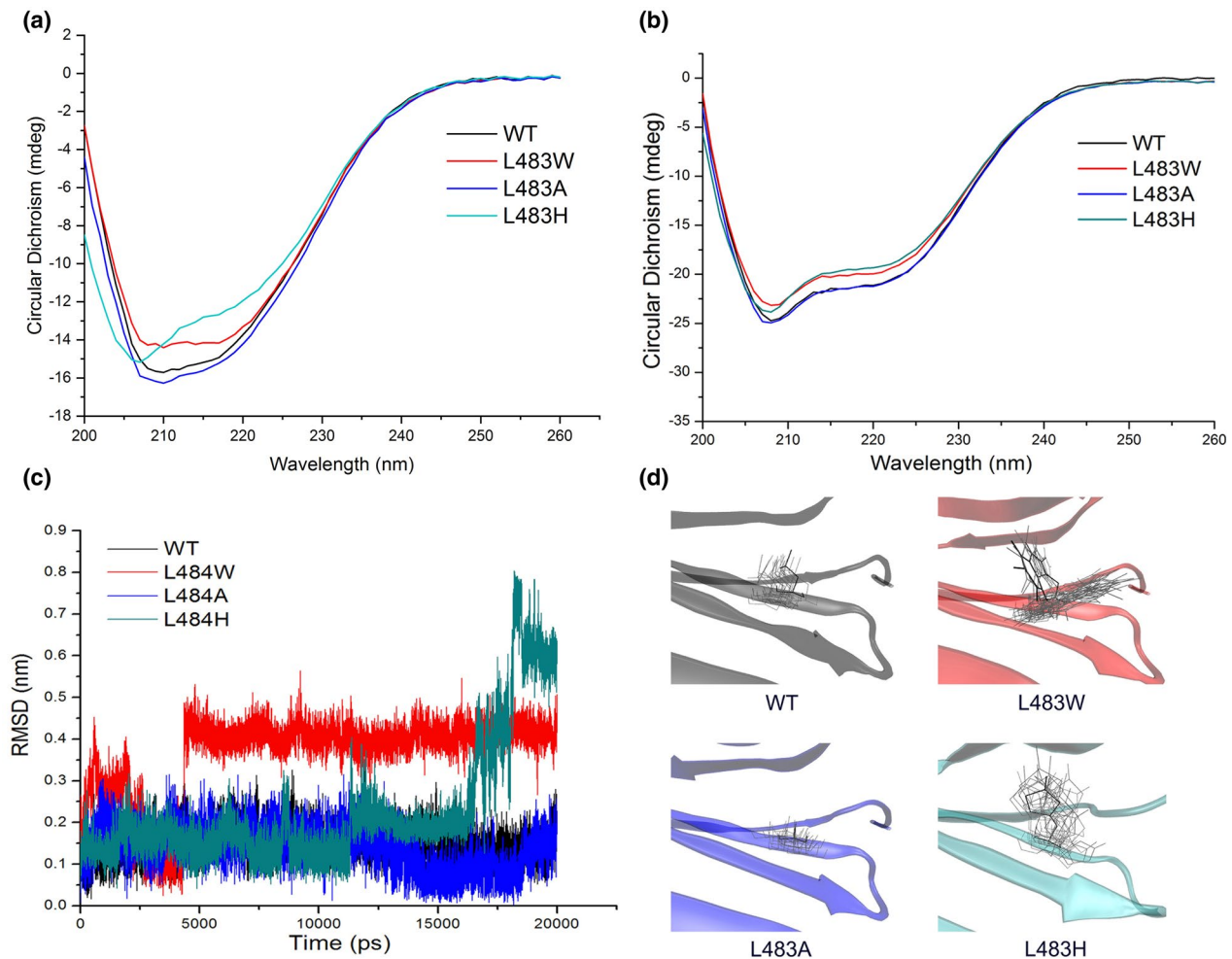
FIGURE 8 Amino acid substitutions at residue 483 alter Hsp70 SBDβ conformation and stability. (a) CD spectra of SBD truncation proteins at 30°C. (b) Secondary structure monitored by far-UV CD for full-length Ssa1 at 30°C. (c) RMSD (root-mean-square deviation) of the side chain of 483 as a function of simulation. (d) Superposition of residue 483 snapshots of every 1 ns during simulations. The 0 ns point is highlighted in bold black [Colour figure can be viewed at wileyonlinelibrary.com]

boundaries are reached, there is a dramatic change in function and resulting phenotype. This is seen in the loss of prion propagation and thermotolerance through replacement of hydrophobic Phe with very small hydrophobic Ala, and with loss of viability due to replacement of Phe/Tyr with extremely large Trp (Table 1). Similar to 475, a proper size of hydrophobic side chain is the key factor for functional change at residue 483. Replacement of hydrophobic Leu with either hydrophilic His or extremely large Trp, resulted in loss of [*PSI*⁺] propagation and reduced thermotolerance (Figure 7a), while replacement with small Ala seems enough to fill the cavity occupied by small Lue in wile-type protein (Figure 7a).

While Cys and Ser are both polar residue and are similar in size , which can result in substitutions displaying similar phenotypic outcomes (Vivian et al., 2003). However, Cys is much more hydrophobic than Ser and has resulted in differing effects through altering protein conformation and thermostability (Lee et al., 2015; Loyola et al., 1999). In this study, F475C displayed a dramatically different prion propagation and thermotolerance compared with F475S

(Figure 3a,b,d). Notably, F475C has a very low abundance like F475S, which suggests a problem with stability (Figure 6b). However, F475C maintains the folding of SBD well (Figure 4a,c), and appears stable after a 24 hr incubation at RT in vitro (Figure 4b). It is possible that F475C causes instability through a mechanism independent from disruption of the SBD. Moreover, cellular functions of Ssa1, such as intrinsic or stimulated ATPase activity (Figure 5b,c) and refolding activity (Figure 6a), are intact in F475C variant, suggesting that F475C may have enhanced chaperone functions, which could compensate for lower abundance. It is clear that the introduction of C at the 475 residue causes a complex change to the in vitro and in vivo properties of Ssa1 that we cannot yet fully appreciate and explain in terms of the phenotypic consequences.

Structural analysis of 475 and 483 mutants suggests that changes in amino acid side chain size at these sites results in major conformational changes in the SBDβ sub-domain and some conformational change in key regions of the NBD (Figures 4a–d and 8a–d). We propose that the steric structural constraints within this critical region

of the SBD are breached by the introduction of amino acids with hydrophilic or larger hydrophobic side chains than the evolutionary conserved Phe475 or Leu483. Structural disturbance in the β6/β7 region causes localised unfolding of this region that spreads into the binding site and also into the NBD-SBD interface. The consequence of unfolding of the SBD is to instigate Hsp70 degradation from the C-terminal region (Xu et al., 2017).

Many ubiquitination sites have been identified on Hsp70 (Peng et al., 2003; Swaney et al., 2013). Parkin mediates the mono-ubiquitination of Hsp70, but fails to alter its steady-state level and promote its proteasomal degradation (Moore et al., 2008). However, CHIP (an E3 ubiquitin protein ligase that binds to the carboxy terminus of Hsp70) is capable of targeting Hsp70/Hsc70 for ubiquitination, and results in rapid 26S proteasome-dependent degradation in vitro (Qian et al., 2006). Notably, Hsp70 was much more susceptible to CHIP-mediated proteasome-dependent degradation, whereas only modest degradation was observed for Hsc70 (Qian et al., 2006), suggesting other E3 ligases target constitutive Hsc70 to trigger proteasome-dependent degradation, or that Hsc70 degradation can occur through another pathway. Additionally, it has been shown that wild-type Ssa1 is rapidly digested into smaller forms, which represents species lacking the whole SBD or the C-terminal lid, and studies indicate that the 45 kDa NBD of Hsp70 is protease resistant whereas the smaller SBD is proteolytically labile (Buchberger et al., 1995; Needham & Masison, 2008). Recently, we showed that Ssa1 denaturation was triggered through unfolding in the β6/7 region of the SBD and induces protein degradation (Xu et al., 2017). An interesting finding from this study is that the SBD cleavage/degradation of Hsp70-Ssa1 appears to be Pep4-dependent (Figure 2a–c). It has not previously been reported that Ssa1 is transported into the vacuole or is a substrate of Pep4. While the possibility exists of complications in protein stabilty during the cleavage assay, the clear genetic evidence presented in Figure 2c, suggests this hypothesis is worthy of further investigation.

The proteasome-dependent proteolytic machinery prevents the accumulation of misfolded proteins during heat shock in eukaryotic cells (Goldberg, 2003). A previous study demonstrated that CHIP mediates a competitive relationship between Hsp70 and misfolded proteins following heat shock by preferentially ubiquitinating chaperone-bound substrates rather than chaperones themselves (Qian et al., 2006). Therefore, Hsp70 exists as a stable long lived protein (half-life of 20.2 hr) (Christiano et al., 2014) and the substrate-bound protein is predominantly degraded (Qian et al., 2006). However, proteasome-dependent degradation is not conserved within all domains of life, which highlights the importance of carboxypeptidase-dependent protein degradation. Intriguingly, there is no CHIP in yeast, so Ssa1 and its misfolded clients may be degraded through other pathways. Additionally, we found that elevated growth temperatures induce instability in the SBD (Xu et al., 2017), and cleavage of this domain can be observed following a 2 hr heat shock (Figure 5d). A plausible explanation is that heat shock disrupts the folding of SBD and exposes the cleavage site to proteinases which leads to further

degradation. It is also possible that Ssa1 binding with misfolding substrates accumulated from heat shock, and co-degraded with substrates through a vacuolar-dependent process.

The prion propagation and thermotolerance phenotypes of the assessed Phe475 and Leu483 mutants correlate well with the extent of SBD instability each mutant produces, that is, the greater structural instability within the SBD, the more severe the loss of function phenotype. A good correlation is also observed when comparing phenotype with biochemical activity. A trend observed for all Hsp70 mutants that impair prion propagation is an increase in basal ATPase activity with a reduced stimulation following addition of either Hsp40 or peptide (Figures 5a–c and 7c) (Needham & Masison, 2008). Dysregulation of ATP hydrolysis will result in an uncoordinated action of the NBD and SBD that will impair Hsp70 function. Genetic evidence for this hypothesis comes from the fact that Hsp70 mutants predicted to affect peptide-binding activity can suppress the prion impairment phenotype of L483W (Jones & Masison, 2003), and it is further supported by steered molecular dynamics simulations (Xu et al., 2013). Additionally, we found that mutants with deficiency in luciferase refolding, had the most severe prion propagation (Figures 6a and 7b).

We find that there is no difference in the abundance of Hsp104 or Ydj1 in any of these mutant strains (Figures 6b and 7d). However, there is variation in the abundance of Ssa1, with F475S, F475C, L483W, and L483H, having low levels of cytosolic Hsp70 (Figures 6b and 7d). Very low levels of Hsp70 in both prion impaired and prion proficient yeast cells has been observed previously with some F475S suppressor mutations restoring protein abundance levels, and others not (Xu et al., 2017). It is not possible to draw any conclusions regarding the abundance of Hsp70 in yeast and a resulting prion or thermotolerance phenotype. Very low levels of Hsp70 are required to maintain normal cellular function under unstressed conditions in yeast as there is no major growth phenotype for any viable 475 or 483 mutant. It is alteration of specific Hsp70 functions that results in phenotypic change and, as in previous studies (Xu et al., 2017), the prion propagation phenotype is much more sensitive to these changes compared to other important central cellular functions carried out by Hsp70. This is the case as 475 and 483 mutants that cannot propagate [PSI^+], do not exhibit other phenotypes under non-stressed conditions. While prion propagation, protein folding and thermotolerance are inherently dependent on the same functional properties of Hsp70, they are distinguishable due to their differing sensitivity to perturbation of Hsp70 function (Xu et al., 2018).

In this study we provide further evidence to support the hypothesis that the β6/β7 region of the Hsp70 SBD plays a major role in maintaining the structural integrity of the entire domain. We speculate that disruption of the SBD results in an equilibrium shift to the unbound state, which allows the NBD subdomains to rotate to a degree where the catalytic residues in the ATPase active centre reach the optimal position for γ-phosphate cleavage (Mayer & Kityk, 2015). As a consequence, in the 475 and 483 mutants that are destabilized, the SBD inhibition of ATP hydrolysis is abolished. The fact that loss of Hsp70 function causes a gradation

of phenotypic responses, with essential cellular functions being least affected, supports the notion that Hsp70 is a druggable target and the β6/β7 region is a prime location for direct or indirect disruption of Hsp70 function.

CONFLICT OF INTEREST

The authors declare no conflicts of interest.

AUTHOR CONTRIBUTIONS

L.X, D.C and Z.H performed the experiments. L.X produced a first draft of the manuscript. G.W.J, S.P, and S.D conceived the study, designed the experiments, and were responsible for research supervision. G.W.J produced the final draft of the manuscript which was edited and agreed upon by all authors.

DATA AVAILABILITY STATEMENT

All materials used in this study are freely available by request to the corresponding author.

ORCID

Hong Zhang https://orcid.org/0000-0001-9204-2547
Sarah Perrett https://orcid.org/0000-0003-0137-0997
Gary W. Jones https://orcid.org/0000-0002-7565-934X

REFERENCES

Abravaya, K., Myers, M.P., Murphy, S.P. & Morimoto, R.I. (1992) The human heat shock protein hsp70 interacts with HSF, the transcription factor that regulates heat shock gene expression. *Genes & Development*, 6(7), 1153–1164. Available from: doi:https://doi.org/10.1101/gad.6.7.1153.

Bertelsen, E.B., Chang, L, Gestwicki, J.E. & Zuiderweg, E.R. (2009) Solution conformation of wild-type *E. coli* Hsp70 (DnaK) chaperone complexed with ADP and substrate. *Proceedings of the National Academy of Sciences of the United States of America*, 106(21), 8471–8476. Available from: doi:https://doi.org/10.1073/pnas.0903503106.

Bertelsen, E.B., Zhou, H., Lowry, D.F., Flynn, G.C. & Dahlquist, F.W. (1999) Topology and dynamics of the 10 kDa C-terminal domain of DnaK in solution. *Protein Science*, 8(2), 343–354. Available from: doi:https://doi.org/10.1110/ps.8.2.343.

Bettencourt, B.R., Feder, M.E. & Cavicchi, S. (1999) Experimental evolution of Hsp70 expression and thermotolerance in drosophila melanogaster. *Evolution*, 53(2), 484–492.

Buchberger, A., Theyssen, H., Schroder, H., McCarty, J.S., Virgallita, G., Milkereit, P. *et al*. (1995) Nucleotide-induced conformational changes in the ATPase and substrate binding domains of the DnaK chaperone provide evidence for interdomain communication. *Journal of Biological Chemistry*, 270(28), 16903–16910. Available from: doi:https://doi.org/10.1074/jbc.270.28.16903.

Calloni, G., Chen, T., Schermann, S.M., Chang, H.C., Genevaux, P., Agostini, F. *et al*. (2012) DnaK functions as a central hub in the *E. coli* chaperone network. *Cell Reports*, 1(3), 251–264.

Chernoff, Y.O., Lindquist, S.L., Ono, B., Inge-Vechtomov, S.G. & Liebman, S.W. (1995) Role of the chaperone protein Hsp104 in propagation of the yeast prion-like factor [psi+]. *Science*, 268(5212), 880–884. Available from: doi:https://doi.org/10.1126/science.7754373.

Christiano, R., Nagaraj, N., Frohlich, F. & Walther, T.C. (2014) Global proteome turnover analyses of the Yeasts *S. cerevisiae* and *S. pombe*. *Cell Reports*, 9(5), 1959–1965.

Flaherty, K.M., DeLuca-Flaherty, C. & McKay, D.B. (1990) Three-dimensional structure of the ATPase fragment of a 70K heat-shock cognate protein. *Nature*, 346(6285), 623–628. Available from: doi:https://doi.org/10.1038/346623a0.

Goldberg, A.L. (2003) Protein degradation and protection against misfolded or damaged proteins. *Nature*, 426(6968), 895–899. Available from: doi:https://doi.org/10.1038/nature02263.

Gong, W., Hu, W., Xu, L., Wu, H., Wu, S., Zhang, H. *et al*. (2018) The C-terminal GGAP motif of Hsp70 mediates substrate recognition and stress response in yeast. *Journal of Biological Chemistry*. Available from: doi:https://doi.org/10.1074/jbc.RA118.002691.

Guex, N. & Peitsch, M.C. (1997) SWISS-MODEL and the Swiss-PdbViewer: an environment for comparative protein modeling. *Electrophoresis*, 18(15), 2714–2723. Available from: doi:https://doi.org/10.1002/elps.1150181505.

Gupta, A., Puri, A., Singh, P., Sonam, S., Pandey, R. & Sharma, D. (2018) The yeast stress inducible Ssa Hsp70 reduces alpha-synuclein toxicity by promoting its degradation through autophagy. *PLoS Genetics*, 14(10), e1007751.

Jones, G.W. & Masison, D.C. (2003) Saccharomyces cerevisiae Hsp70 mutations affect [PSI+] prion propagation and cell growth differently and implicate Hsp40 and tetratricopeptide repeat cochaperones in impairment of [PSI+]. *Genetics*, 163(2), 495–506.

Jones, G., Song, Y., Chung, S. & Masison, D.C. (2004) Propagation of *Saccharomyces cerevisiae* [PSI+] prion is impaired by factors that regulate Hsp70 substrate binding. *Molecular and Cellular Biology*, 24(9), 3928–3937. Available from: doi:https://doi.org/10.1128/MCB.24.9.3928-3937.2004.

Jones, G.W. & Tuite, M.F. (2005) Chaperoning prions: the cellular machinery for propagating an infectious protein? *BioEssays*, 27(8), 823–832. Available from: doi:https://doi.org/10.1002/bies.20267.

Jung, G., Jones, G., Wegrzyn, R.D. & Masison, D.C. (2000) A role for cytosolic hsp70 in yeast [PSI(+)] prion propagation and [PSI(+)] as a cellular stress. *Genetics*, 156(2), 559–570.

Kityk, R., Vogel, M., Schlecht, R., Bukau, B. & Mayer, M.P. (2015) Pathways of allosteric regulation in Hsp70 chaperones. *Nature Communications*, 6, 8308. https://doi.org/10.1038/ncomms9308

Lee, D.H. & Goldberg, A.L. (1996) Selective inhibitors of the proteasome-dependent and vacuolar pathways of protein degradation in *Saccharomyces cerevisiae*. *Journal of Biological Chemistry*, 271(44), 27280–27284.

Lee, E.M., Lee, S.S., Tripathi, B.N., Jung, H.S., Cao, G.P., Lee, Y. *et al*. (2015) Site-directed mutagenesis substituting cysteine for serine in 2-Cys peroxiredoxin (2-Cys Prx A) of Arabidopsis thaliana effectively improves its peroxidase and chaperone functions. *Annals of Botany*, 116(4), 713–725.

Loovers, H.M., Guinan, E. & Jones, G.W. (2007) Importance of the Hsp70 ATPase domain in yeast prion propagation. *Genetics*, 175(2), 621–630. Available from: doi:https://doi.org/10.1534/genetics.106.066019.

Lotz, S.K., Knighton, L.E., Nitika, J.G.W. & Truman, A.W. (2019) Not quite the SSAme: unique roles for the yeast cytosolic Hsp70s. *Current Genetics*, 65(5), 1127–1134. Available from: doi:https://doi.org/10.1007/s00294-019-00978-8.

Loyola, C., Saavedra, C., Gomez, I. & Vasquez, C. (1999) The amino acidic substitution of cysteine 167 by serine (C167S) in BstVI restriction endonuclease of Bacillus stearothermophilus V affects its conformation and thermostability. *Biochimie*, 81(3), 261–266. Available from: doi:https://doi.org/10.1016/S0300-9084(99)80060-1.

Mandal, S.S., Merz, D.R., Buchsteiner, M., Dima, R.I., Rief, M. & Zoldak, G. (2017) Nanomechanics of the substrate binding domain of Hsp70 determine its allosteric ATP-induced conformational change. *Proceedings of the National Academy of Sciences of the United States of America*, 114(23), 6040–6045. Available from: doi:https://doi.org/10.1073/pnas.1619843114.

Masison, D.C., Kirkland, P.A. & Sharma, D. (2009) Influence of Hsp70s and their regulators on yeast prion propagation. *Prion*, 3(2), 65–73. Available from: doi:https://doi.org/10.4161/pri.3.2.9134.

Matveenko, A.G., Barbitoff, Y.A., Jay-Garcia, L.M., Chernoff, Y.O. & Zhouravleva, G.A. (2018) Differential effects of chaperones on yeast prions: CURrent view. *Current Genetics*, 64(2), 317–325. Available from: doi:https://doi.org/10.1007/s00294-017-0750-3.

Mayer, M.P. & Gierasch, L.M. (2019) Recent advances in the structural and mechanistic aspects of Hsp70 molecular chaperones. *Journal of Biological Chemistry*, 294(6), 2085–2097. Available from: doi:https://doi.org/10.1074/jbc.REV118.002810.

Mayer M.P., Kityk R. (2015) Insights into the molecular mechanism of allostery in Hsp70s. *Frontiers in Molecular Biosciences*, 2 http://dx.doi.org/10.3389/fmolb.2015.00058.

Mayer, M.P., Schroder, H., Rudiger, S., Paal, K., Laufen, T. & Bukau, B. (2000) Multistep mechanism of substrate binding determines chaperone activity of Hsp70. *Natural Structural Biology*, 7(7), 586–593.

Moore, D.J., West, A.B., Dikeman, D.A., Dawson, V.L. & Dawson, T.M. (2008) Parkin mediates the degradation-independent ubiquitination of Hsp70. *Journal of Neurochemistry*, 105(5), 1806–1819. Available from: doi:https://doi.org/10.1111/j.1471-4159.2008.05261.x.

Morimoto, R.I. & Santoro, M.G. (1998) Stress-inducible responses and heat shock proteins: New pharmacologic targets for cytoprotection. *Nature Biotechnology*, 16(9), 833–838. Available from: doi:https://doi.org/10.1038/nbt0998-833.

Needham, P.G. & Masison, D.C. (2008) Prion-impairing mutations in Hsp70 chaperone Ssa1: effects on ATPase and chaperone activities. *Archives of Biochemistry and Biophysics*, 478(2), 167–174. Available from: doi:https://doi.org/10.1016/j.abb.2008.07.023.

O'Brien, M.C. & McKay, D.B. (1993) Threonine 204 of the chaperone protein Hsc70 influences the structure of the active site, but is not essential for ATP hydrolysis. *Journal of Biological Chemistry*, 268(32), 24323–24329.

Panaretou, B. & Jones, G.W. (2014) Yeast models for amyloid disease. *Essays in Biochemistry*, 56, 85–97. Available from: doi:https://doi.org/10.1042/bse0560085.

Peng, J., Schwartz, D., Elias, J.E., Thoreen, C.C., Cheng, D., Marsischky, G. *et al.* (2003) A proteomics approach to understanding protein ubiquitination. *Nature Biotechnology*, 21(8), 921–926. Available from: doi:https://doi.org/10.1038/nbt849.

Qian, S.B., McDonough, H., Boellmann, F., Cyr, D.M. & Patterson, C. (2006) CHIP-mediated stress recovery by sequential ubiquitination of substrates and Hsp70. *Nature*, 440(7083), 551–555. Available from: doi:https://doi.org/10.1038/nature04600.

Rowlands, M.G., Newbatt, Y.M., Prodromou, C., Pearl, L.H., Workman, P. & Aherne, W. (2004) High-throughput screening assay for inhibitors of heat-shock protein 90 ATPase activity. *Analytical Biochemistry*, 327(2), 176–183. Available from: doi:https://doi.org/10.1016/j.ab.2003.10.038.

Sharma, D. & Masison, D.C. (2008) Functionally redundant isoforms of a yeast Hsp70 chaperone subfamily have different antiprion effects. *Genetics*, 179(3), 1301–1311. Available from: doi:https://doi.org/10.1534/genetics.108.089458.

Sondheimer, N., Lopez, N., Craig, E.A. & Lindquist, S. (2001) The role of Sis1 in the maintenance of the [RNQ+] prion. *EMBO Journal*, 20(10), 2435–2442. Available from: doi:https://doi.org/10.1093/emboj/20.10.2435.

Stevens, S.Y., Cai, S., Pellecchia, M. & Zuiderweg, E.R. (2003) The solution structure of the bacterial HSP70 chaperone protein domain DnaK(393–507) in complex with the peptide NRLLLTG. *Protein Science*, 12(11), 2588–2596. Available from: doi:https://doi.org/10.1110/ps.03269103.

Swaney, D.L., Beltrao, P., Starita, L., Guo, A., Rush, J., Fields, S. *et al.* (2013) Global analysis of phosphorylation and ubiquitylation cross-talk in protein degradation. *Nature Methods*, 10(7), 676–682. Available from: doi:https://doi.org/10.1038/nmeth.2519.

Tyedmers, J., Mogk, A. & Bukau, B. (2010) Cellular strategies for controlling protein aggregation. *Nature Reviews Molecular Cell Biology*, 11(11), 777–788. Available from: doi:https://doi.org/10.1038/nrm2993.

Van Der Spoel, D., Lindahl, E., Hess, B., Groenhof, G., Mark, A.E. & Berendsen, H.J. (2005) GROMACS: fast, flexible, and free. *Journal of Computational Chemistry*, 26(16), 1701–1718. Available from: doi:https://doi.org/10.1002/jcc.20291.

Verghese, J., Abrams, J., Wang, Y. & Morano, K.A. (2012) Biology of the heat shock response and protein chaperones: Budding yeast (*Saccharomyces cerevisiae*) as a model system. *Microbiology and Molecular Biology Reviews*, 76(2), 115–158. Available from: doi:https://doi.org/10.1128/MMBR.05018-11.

Vivian, J.P., Hastings, A.F., Duggin, I.G., Wake, R.G., Wilce, M.C. & Wilce, J.A. (2003) The impact of single cysteine residue mutations on the replication terminator protein. *Biochemical and Biophysical Research Communications*, 310(4), 1096–1103. Available from: doi:https://doi.org/10.1016/j.bbrc.2003.09.126.

Wickner, R.B. (1994) [URE3] as an altered URE2 protein: evidence for a prion analog in Saccharomyces cerevisiae. *Science*, 264(5158), 566–569. Available from: doi:https://doi.org/10.1126/science.7909170.

Wickner, R.B. & Masison, D.C. (1996) Evidence for two prions in yeast: [URE3] and [PSI]. *Current Topics in Microbiology and Immunology*, 207, 147–160.

Xu, L., Gong, W., Cusack, S.A., Wu, H., Loovers, H.M., Zhang, H. *et al.* (2017) The beta6/beta7 region of the Hsp70 substrate-binding domain mediates heat-shock response and prion propagation. *Cellular and Molecular Life Sciences.* 75(8), 1445–1459.

Xu, L., Gong, W., Zhang, H., Perrett, S. & Jones, G.W. (2018) The same but different: The role of Hsp70 in heat shock response and prion propagation. *Prion*, 12(3–4), 170–174. Available from: doi:https://doi.org/10.1080/19336896.2018.1507579.

Xu, L., Hasin, N., Shen, M., He, J., Xue, Y., Zhou, X. *et al.* (2013) Using steered molecular dynamics to predict and assess Hsp70 substrate-binding domain mutants that alter prion propagation. *PLoS Computational Biology*, 9(1), e1002896. Available from: doi:https://doi.org/10.1371/journal.pcbi.1002896.

Xu, L., Nitika, H.N., Cuskelly, D.D., Wolfgeher, D., Doyle, S. *et al.* (2019) Rapid deacetylation of yeast Hsp70 mediates the cellular response to heat stress. *Scientific Reports*, 9(1), 16260. https://doi.org/10.1038/s41598-019-52545-3

Zhu, X., Zhao, X., Burkholder, W.F., Gragerov, A., Ogata, C.M., Gottesman, M.E. *et al.* (1996) Structural analysis of substrate binding by the molecular chaperone DnaK. *Science*, 272(5268), 1606–1614. https://doi.org/10.1126/science.272.5268.1606

SUPPORTING INFORMATION

Additional Supporting Information may be found online in the Supporting Information section.